Biomedicine & Pharmacotherapy 167 (2023) 115612

Contents lists available at ScienceDirect

Biomedicine & Pharmacotherapy

journal homepage: www.elsevier.com/locate/biopha

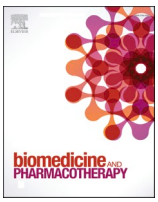

Hepatocyte survival and proliferation by fibroblast growth factor 7 attenuates liver inflammation, and fibrogenesis during acute liver injury via paracrine mechanisms

Eline Geervliet [a,b], Leon W.M.M. Terstappen [c], Ruchi Bansal [a,*]

[a] Translational Liver Research, Department of Medical Cell BioPhysics, Technical Medical Centre, Faculty of Science and Technology, University of Twente, the Netherlands
[b] Institute of Molecular Pathobiochemistry, Experimental Gene Therapy and Clinical Chemistry, RWTH University Hospital Aachen, Germany
[c] Department of Medical Cell BioPhysics, Technical Medical Centre, Faculty of Science and Technology, University of Twente, the Netherlands

ARTICLE INFO

Keywords:
Liver injury
FGF7
FGFR2b
Hepatocyte regeneration
Inflammation and fibrogenesis

ABSTRACT

Hepatocyte damage during liver injury instigates activation of macrophages and hepatic stellate cells (HSCs) resulting in liver inflammation and fibrosis respectively. Improving hepatocyte survival and proliferation thereby ameliorating inflammation and fibrosis represents a promising approach for the treatment of liver injury. In the liver, fibroblast growth factors (FGFs) play a crucial role in promoting hepatocyte proliferation and tissue regeneration. Among 22 FGFs, FGF7 induces hepatocyte survival and liver regeneration as shown previously in mouse models of cholestatic liver injury and partial hepatectomy. We hypothesized that FGF7 promotes hepatocyte survival and proliferation by interacting with FGFR2b, expressed on hepatocytes, and ameliorates liver injury (inflammation and early fibrogenesis) via paracrine mechanisms. To prove this hypothesis and to study the effect of FGF7 on hepatocytes and liver injury, we administered FGF7 exogenously to mice with acute carbon tetrachloride (CCl_4)-induced liver injury. We thereafter studied the underlying mechanisms and the effect of exogenous FGF7 on hepatocyte survival and proliferation, and the consequent paracrine effects on macrophage-induced inflammation, and HSCs activation in vitro and in vivo. We observed that the expression of FGF7 as well as FGFR2 is upregulated during acute liver injury. Co-immunostaining of FGF7 and collagen-I confirmed that FGF7 is expressed by HSCs and is possibly captured by the secreted ECM. Immunohistochemical analysis of liver sections showed increased hepatocyte proliferation upon exogenous FGF7 treatment as determined by Ki67 expression. Mechanistically, exogenous FGF7 improved hepatocyte survival (and increased drug detoxification) via AKT and ERK pathways while maintaining hepatocyte quiescence restricting hepatocarcinogenesis via P27 pathways. Flow cytometry analysis revealed that improved hepatocyte survival and proliferation leads to a decrease in infiltrated monocytes-derived macrophages, as a result of reduced CCL2 (and CXCL8) expression by hepatocytes. Moreover, conditioned medium studies showed reduced collagen-I secretion by HSCs (indicative of HSCs activation) upon treatment with FGF7-treated hepatocytes conditioned medium. Altogether, we show that exogenous administration of FGF7 induces hepatocyte survival and proliferation and leads to amelioration of inflammatory response and fibrosis in acute liver injury via paracrine mechanisms. Our study further demonstrates that FGF7, FGF7 derivatives, or nano-engineered FGF7 may benefit patients with hepatic dysfunction.

1. Introduction

Hepatocyte injury is the onset of acute and chronic liver diseases [1,2]. Upon injury, hepatocytes release paracrine signals i.e., pro-inflammatory cytokines and chemokines (hepatokines) initiating resident Kupffer cell (KC) activation, and infiltration of bone marrow-derived monocytes respectively causing liver inflammation [3]. Continuous hepatocyte injury and persistent inflammation lead to the release of pro-fibrotic hepatokines by damaged hepatocytes and cytokines/chemokines by immune cells activating quiescent hepatic stellate

* Correspondence to: Translational Liver Research, Department of Medical Cell BioPhysics, Technical Medical Centre, Faculty of Science and Technology, University of Twente, Carre 4419, Drienerlolaan 5, 7522NB Enschede, the Netherlands.
E-mail address: r.bansal@utwente.nl (R. Bansal).

https://doi.org/10.1016/j.biopha.2023.115612
Received 8 August 2023; Received in revised form 18 September 2023; Accepted 27 September 2023
Available online 3 October 2023

cells (HSCs) that produce excessive amounts of extracellular matrix (ECM) components, mainly collagen-I, inducing liver scarring referred to as fibrosis [4]. Over recent years, several therapeutic strategies have been explored that include the removal of the underlying cause of hepatocyte injury or promoting hepatocyte regeneration, inhibition in monocyte infiltration or inactivation of pro-inflammatory macrophages/activation of anti-inflammatory macrophages, elimination or inactivation of activated HSCs, or degradation of ECM [5–9]. Liver transplantation remains the only treatment option for (end-stage) liver diseases however possesses several challenges such as limited donor livers and life-long immunosuppressants [10,11]. Hence, there is an urgent need for (new) therapies.

It is believed that hepatocyte damage as a consequence of injury, necrosis, and lack of proliferation is the cause of liver disease progression [12,13]. Lee et al., indicated that full liver transplantation is not necessary as long as proliferating hepatocytes are transplanted, explaining hepatocyte capacity to proliferate is essential to success [14]. Concomitantly, novel therapeutics promoting hepatocyte proliferation show promising results [15]. In the liver, fibroblast growth factors (FGFs) play a crucial role in promoting hepatocyte proliferation and tissue regeneration [16]. FGFs are proteins involved in embryonic development, cell survival and proliferation, and progenitor cell differentiation. Until now, 22 FGFs have been discovered that are subdivided into seven subfamilies: FGF1 (FGF1/2), FGF4 (FGF4/5/6), FGF7 (FGF3/7/10/22), FGF8 (FGF8/17/18), FGF9 (FGF9/16/20), FGF11 (FGF11/12/13/14) and FGF19 (FGF19/21/23). FGFs can bind to one or more of the 4 FGF receptors (FGFRs), FGFR1–4, to induce their functions [17]. Lack of one or more FGFs or FGFRs, during partial hepatectomy or hepatic injury, evidenced diminished or total lack of liver regeneration, indicating their vital role in liver regeneration [16,18]. Several FGFs, FGF analogues, and FGFR agonists (and antagonists) are being evaluated in ameliorating hepatic fibrosis, promoting hepatic repair, and/or interfering with hepatocarcinogenesis [17]. These FGF subfamilies, along with their corresponding FGFRs, constitute a complex network of signalling pathways in the liver. Understanding their specific roles can lead to the development of targeted therapies for various liver diseases, offering new hope for patients and improving liver health outcomes.

In our previous study, we have shown that liver-specific delivery of FGF2 using superparamagnetic iron oxide nanoparticles attenuated HSC activation and early liver fibrogenesis in vivo [19]. In this study, we focused our attention on FGF7, a paracrine FGF that belongs to the FGF7 subfamily. FGF7, also known as keratinocyte growth factor (KGF), is an FGF that binds exclusively to FGFR2-IIIb, expressed on hepatocytes [17]. FGF7-knockout studies have revealed that FGF7 is essential for cell survival and proliferation of hepatocytes (and expansion of liver progenitor cells) [20]. Furthermore, FGF7 upregulates detoxifying enzymes in the liver [18], and has shown protective effects in cholestatic liver injury [21,22]. Importantly, FGFR2-IIIb is downregulated in HCC while re-expression correlated with reduced tumorigenicity independent of FGF7 [23] suggesting exogenous FGF7 will not affect tumor progression. Altogether FGF7, via interaction with FGFR2b, protects hepatocytes from injury and promotes hepatocyte regeneration without affecting hepatocarcinogenesis. During liver injury, FGF7 is secreted by HSCs [24] while FGFR2-IIIb is expressed on hepatocytes [21]. We hypothesize that FGF7 promotes hepatocyte survival and proliferation by interacting with FGFR2b, expressed on hepatocytes, and ameliorates liver injury (inflammation and early fibrogenesis) via paracrine mechanisms. To prove this hypothesis and to study the effect of FGF7 on liver injury, we administered FGF7 exogenously to mice with acute carbon tetrachloride (CCl_4)-induced liver injury. We thereafter studied the underlying mechanisms and the effect of exogenous FGF7 on hepatocyte survival and proliferation, and the consequent paracrine effects on macrophage-induced inflammation, and HSCs activation in vitro and in vivo.

2. Materials and methods

2.1. Materials

Carbon tetrachloride (CCl_4) (Cat. no. 02671, Sigma Aldrich, St. Louis, MO, USA); olive oil (Cat. no. O1514, Sigma Aldrich); (2-Hydroxypropyl)-β-cyclodextrin (Cat. no. 778966, Sigma Aldrich); Kolliphor HS15 (Cat. no. 42966, Sigma Aldrich); FGF7 (Cat. no. NBP2–35149 Novus biologicals, Zillow, CO, USA); Roswell Park Memorial Institute (RPMI) 1640 with L-Glutamine (Capricorn Scientific, Ebsdorfergrund, Germany); Penicillin/Streptomycin, (Capricorn Scientific); Bovine Serum Albumin (BSA) (Cat. no. A7906, Sigma Aldrich); Fetal Bovine Serum (FBS) (Cat. no. F7524, Sigma Aldrich); Phosphate Buffered Saline (PBS) tablets (Cat. no. 524650, Millipore, Watford, UK); Formaldehyde (Cat. no. F8775, Sigma Aldrich); Hoechst 33342, Trihydrochloride, Trihydrate (Cat. no. H1399, Thermo Fisher Scientific, Wesel, Germany); Epredia Cryomatrix™ embedding resin (Cat. no. 6769006, Epredia, Runcorn, UK); 2-methylbutane (Cat. no. M32631, Sigma Aldrich); 3-Amino-9-ethylcarbazole (AEC) (Cat. no. A6926, Sigma Aldrich); Fluoroshield with 4′,6-Diamidino-2-phenylindole dihydrochloride (DAPI) (Cat. no. F6057, Sigma Aldrich); Dimethylformamide (DMF) (Cat. no. 227056, Sigma Aldrich); Haematoxylin solution according to Mayer (Cat. no. 51275, Sigma Aldrich); Aqueous Mounting Medium Aquatex (Cat. no. 1085620050, Sigma Aldrich); SV Total RNA Isolation System (Cat. no. Z3105, Promega, Leiden, Netherlands); iScript cDNA synthesis kit (Cat. no. 1708891, BioRad, Lunteren, Netherlands); SensiMix Plus SYBR & Fluorescein (Cat. no. QT615–20, GC biotech, Waddinxveen, Netherlands); Dulbecco's Modified Eagle Medium (DMEM) High Glucose (4.5 g/L) with L-Glutamine (Capricorn Scientific); Acetaminophen (APAP) (Cat. no. A-7085, Sigma Aldrich); Alamar blue (resazurin sodium salt) (Cat. no. 199303, VWR, Langenfeld, Germany); Recombinant FGF7 (Cat. no. NBP2–3514, Novus biologicals); DMEM, high glucose, GlutaMAX™ Supplement, HEPES (Cat. no. 11584456, Thermo Fisher Scientific); Universal RNA kit (Cat. no. E3598–02, Roboklon, Berlin, Germany).

2.2. CCl_4-induced acute liver injury mouse model

All the animal experiments were carried out according to the ethical guidelines for the Care and Use of Laboratory Animals (Utrecht University, The Netherlands). CCl_4 was prepared in olive oil (0.2 mL/kg) and FGF7 (50 μg/kg) was prepared in (2-Hydroxypropyl)-β-cyclodextrin (10 %) + Kolliphor HS15 (5 %) in MilliQ (85 %). Male C57BL/6 mice (10–12 weeks old) received a single intraperitoneal (IP) injection of olive oil (healthy, n = 12) or 0.2 mL/kg CCl_4 (n = 24) on day 1. On days 2 and 3, the CCl_4-treated mice received vehicle [(2-Hydroxypropyl)-β-cyclodextrin (10 %) + Kolliphor HS15 (5 %) in MilliQ (85 %), n = 12] or 50 μg/kg FGF7 (n = 12) twice daily intraperitoneally. On day 4, all the animals were euthanized. The liver, lungs, kidneys, spleen, and heart were harvested, weighed, and processed for further analysis. Total aspartate transferase (AST) levels were measured in the plasma as per standard biochemical assays.

2.3. Immunohistochemical staining

Liver tissues were harvested and transferred to cryomatrix, and snap-frozen in 2-methylbutane chilled on dry ice. Cryosections (6 μm) were made using a Leica CM 1860 cryostat (Leica Microsystems, Nussloch, Germany). The sections were air-dried and fixed with acetone for 20 min at room temperature. Thereafter, tissue cryosections were rehydrated in PBS and incubated with the primary antibody listed in supplementary Table 1 at 4 °C overnight. The next day, sections were washed 3 times in PBS. Endogenous peroxidase activity was blocked by 0.3 % H_2O_2 prepared in methanol for 30 min. Sections were washed 3 times in PBS and then incubated with horseradish peroxidase (HRP)-conjugated secondary antibody (listed in Supplementary Table 1) for 1 h at room

temperature. Thereafter, sections were washed 3 times in PBS and incubated with HRP-conjugated tertiary antibody (Supplementary Table 1) for 1 h at room temperature and again washed 3 times in PBS. AEC solution was freshly prepared by combining 4.5 mL MilliQ, 500 μL 1 M sodium acetate pH 5.5, and 250 μL 3-Amino-9-ethylcarbazole (AEC) in dimethylformamide (DMF) (1 tablet per 2.5 mL DMF). This was filtered using a 4.5 μm nylon filter and 5.2 μL 30 % H_2O_2 was added before use. Peroxidase activity was developed using an AEC solution for 20 min at RT, and nuclei were counterstained with haematoxylin for 5 min. After 5 min of washing under tap water, sections were mounted in Aquatex mounting medium. Slides were digitized using a NanoZoomer 2.0 HT whole slide scanner (Hamamatsu, Shizuoka, Japan), and resulting digital images were visualized at 1680 × 1050-pixel resolution with NDP software and analysed using FIJI/ImageJ software.

2.4. Immunofluorescent staining

Immunofluorescent staining was performed similar to immunohistochemistry staining for Collagen-I, FGF7, FGFR2, and Ki-67: after overnight incubation with primary antibody, cells were washed 3 times with PBS and incubated with Alexa Fluor (AF)488 or AF594-conjugated secondary antibody (see Supplementary Table 1) for 1 h at room temperature. For Albumin: after rehydrated in PBS, liver sections were incubated with the albumin biotinylated detection antibody listed in Supplementary Table 1 at 4 °C overnight. The next day, sections were washed 3 times in PBS and incubated with FITC streptavidin (BioLegend, San Diego, California, USA) for 1 h at room temperature. After 1 h, all sections were washed 3 times in PBS and mounted with DAPI mounting medium.

2.5. Mouse apoptosis signalling pathway

For protein isolation, liver tissues were lysed in RIPA buffer and homogenized using the Tekmar Tissumizer Homogenizer (IKA-Werke, Breisgau, Germany). After homogenization, protein content was measured using the Pierce BCA protein assay kit (Thermo Fisher Scientific) as per the manufacturer's instructions. For the assay, multiple samples were combined to perform the apoptosis assay to have representative results. For CCl_4 and CCl_4 +FGF7 mice, all 12 samples were paired and analysed, for healthy controls, 10 samples were paired and analysed. Apoptosis assay analysis was performed using RayBio® C-series mouse apoptosis signalling pathway array (RayBiotech, Norcross, GA, USA) as per the manufacturer's instructions (see Supplementary Fig. S1). Results were analysed with AzureSpot Analysis Software (Azure Biosystems, Dublin, CA, USA).

2.6. Preparation of cell suspension and flow cytometric analysis

Freshly collected liver tissues were mechanically ground using the TissueGrinder (TG, Fast Forward Discoveries GmbH, Mannheim, Germany). Liver tissue pieces (approximately 30 mg) from all liver lobes were cut into small pieces and put in 1 mL RPMI 1640 with L-Glutamine supplemented with 1 % Penicillin/Streptomycin and 1 % Bovine Serum Albumin (referred to as RPMI-TG-medium) in a 12-wells plate, which was put on ice until processing. Tissues were then transferred into the rotor unit of the 50 mL Falcon® Tube (TG-C-100, Fast Forward Discoveries) with 750 μL RPMI-TG-medium and the TG Falcon tube was assembled as per manufacturer's instructions. The tube was positioned in the TG device and an optimized protocol for liver dissociation provided by the manufacturer was used. After grinding, the tube was centrifuged for 5 min at 300 g. The cells were washed 3 times with 1 mL PBS containing 2 % FBS. Cells were fixed with 4 % formaldehyde prepared in PBS with 2 % FBS for 30 min. Cells were washed 3 times with 1 mL PBS with 2 % FBS, stained, and analysed within 7 days. Cells were stained with 100 μL containing 1 μL fluorescent antibodies (listed in Supplementary Table 2) for 1 h and Hoechst 33342 (10 μg/100 μL) was added for 30 min. Cells were washed 3 times with 1 mL PBS with 2 % FBS. Cells were identified using flow cytometry (BD FACS Aria II BD, Bioscience, San Jose, CA), and the data was analysed using FlowJo v10.7.0 (Tree Star, Inc., Ashland, OR).

Gating strategy (see Supplementary Fig. S2): Cells were visualized on an SSC/FSC plot (step 1). For the identification of the infiltrated monocyte-derived macrophages (MoMFs), we first excluded all the debris and other non-nuclear events using Hoechst (step 2). All Hoechst positive cells (blue) were subsequently plotted on an SSC/APC plot to identify CD45+ leukocytes (red) by gating the APC-CD45 positive cells (step 3). Thereafter, the CD45+ cells were further investigated on the SSC/APC plot, and lymphocytes and NK-cells (light green) were excluded by excluding the population that has low granularity (SSC) and were CD45++ (step 4). The remaining cells were plotted on a graph with CD11b (y-axis) and F4/80 (x-axis) where the CD11b++, F4/80+/- population was considered as the MoMF population (orange), and CD11b+/- and F4/80++ population was considered as the KC population (dark green) (step 5 and 6).

2.7. Quantitative real-time PCR

Total RNA from liver tissue was isolated using SV Total RNA Isolation System (Promega) as per manufacturer's instruction. The RNA concentration was quantified with a BioSpec-nano Spectrophotometer (Shimadzu Europa GmbH, Duisburg, Germany), and total RNA (1 μg) was reverse transcribed using the iScript cDNA Synthesis Kit. Real-time PCR was performed using 20 ng of cDNA, pre-tested gene-specific primer sets (Sigma Aldrich), listed in Supplementary Table 3 and 2× SensiMix SYBR according to the manufacturer's instructions. PCR was performed in the CFX384 Touch Real-Time PCR Detection System (Bio-Rad). Finally, cycle threshold (Ct) values were normalized to reference gene GAPDH and relative gene expression was calculated using the $2^{-\Delta\Delta Ct}$-method.

2.8. Cell lines

HepG2, an immortalized human hepatocyte cell line (American Type Culture Collection, ATCC, Manassas, Virginia, USA) was cultured in DMEM high Glucose (4.5 g/L), supplemented with 200 mM L-Glutamine, 10 % FBS, 50 U/mL penicillin and 50 μg/mL streptomycin. LX-2, an immortalized human hepatic stellate cell (HSC) line provided by Prof. Scott Friedman (Mount Sinai Hospital, New York, USA), was cultured in DMEM, high-glucose, with GlutaMAX supplemented with 10 % FBS, 50 U/mL penicillin and 50 μg/mL streptomycin. The cells were passaged twice a week as per established experimental protocols.

2.9. In vitro studies on HepG2 cells

Cells were either seeded in 12-well plates (2×10^5 cells/well/mL) (viability and FGFR2b expression) or in 6-well plates (6×10^5 cells/well in 3 mL) (for conditioned medium) and cultured for 24 h. Cells were incubated with medium alone (0 mM APAP) or 10 mM APAP for 24 h, to induce hepatocyte injury. Cells were washed twice with 500 μL PBS and incubated with medium alone (0 ng/mL FGF7) or 50 ng/mL FGF7 for 6 h. For the conditioned medium (see Supplementary Fig. S3), the medium was collected and centrifuged for 3 min at 300 g, to remove (dead) cells. For PCR analysis, cells were washed with 500 μL PBS and lysed with RNA lysis buffer. RNA was isolated using a Universal RNA kit as per the manufacturer's instructions. RNA concentration measurements, cDNA synthesis, and quantitative PCR were performed as described previously. For viability, after 3 h of incubation with FGF7, Alamar blue reagent was added and incubated for the remaining 3 h. After a total of 6 h, 100 μL medium was collected and measured using a Victor X3 plate reader (Perkin Elmer, Waltham, MA, USA).

2.10. In vitro studies on LX-2 cells

FGF7 expression was measured in non-activated and TGFβ-activated LX-2 cells. Cells were seeded in 12-well plates (1×10^5 cells/well in 1 mL) and cultured for 24 h. The next day, cells were serum-starved for 24 h and were incubated with medium alone or with 5 ng/mL TGFβ for 24 h. Cells were washed, and lysed and total mRNA was purified for quantitative PCR analysis as previously described.

For conditioned medium experiments (see supplementary Fig. S3), cells were plated and starved as previously described. After 24 h of starvation, LX-2 cells were incubated with conditioned: fresh medium (2:1) for 24 h. After 24 h, cells were washed with 500 μL PBS and lysed. RNA was isolated and total mRNA was purified for quantitative PCR analysis as previously described.

2.11. Graphs and statistical analysis

All graphs were made, and statistical analysis was performed using GraphPad Prism version 10.0.1 (GraphPad Prism, La Jolla, CA, USA). The results are expressed as the mean + standard error of the mean (SEM). Multiple comparisons between different groups were calculated using the one-way analysis of variance (ANOVA) with the Bonferroni post hoc test. Statistical differences between the two groups were calculated using a two-tailed unpaired t-test. Differences were considered significant when *$p < 0.05$, **$p < 0.01$, ***$p < 0.001$, or ****$p < 0.0001$.

3. Results

3.1. Upregulation of FGF7 and FGFR2 in vitro and in vivo

Previous studies have shown a correlation between FGF7 expression with the fibrosis stage in human livers and mouse livers both at the mRNA and protein level [24,25]. Moreover, increased FGFR2b expression levels are observed during the early stages of liver fibrosis while downregulation in FGFR2b levels is observed in cirrhotic liver tissue possibly due to the loss of hepatocytes and the proportional reduction in FGFR2b [24,25]. In this study, we examined the mRNA expression of *Fgf7* and *FgfR2b* in the livers of mice with CCl_4-induced acute liver injury versus healthy controls. As shown in Fig. 1A, we observed upregulation in *Fgf7* and *FgfR2b* gene expression levels in CCl_4 mice versus healthy controls ($p < 0.05$). We further confirmed the cellular source of FGF7 and FGFR2. As reported earlier [24], we found that FGF7 mRNA expression was increased in TGFβ-activated human HSCs (LX2 cells) ($p < 0.05$) (Fig. 1B). FGFR2b is shown to be exclusively expressed on hepatocytes [24], and the expression is down-regulated in HCC cells and tissues while re-expression induces a higher apoptosis rate and reduced proliferation [26]. Although studies have reported that FGFR2b is upregulated in hepatocytes after partial hepatectomy [20,24,25], none of these studies have analysed the expression of FGFR2b upon hepatocyte injury. In this study, we investigated the expression of FGFR2b in acetaminophen (APAP)-treated human hepatocytes and found decreased mRNA expression of FGFR2-IIIb in acetaminophen (APAP)--treated human hepatocytes (HepG2 cells) versus healthy HepG2 cells (Fig. 1B). This reduced expression of FGFR2b in vitro correlates with reduced FGFR2b expression observed during liver cirrhosis and possibly confers a lower rate of apoptosis and increased proliferation.

We further assessed the protein expression of FGF7 and FGFR2b in CCl_4 mice versus healthy controls and confirmed their co-localization with HSCs and hepatocytes in vivo respectively. We performed co-immunostainings using FGF7 and collagen-I (HSCs); and FGFR2b and albumin (hepatocytes). Fig. 1C-D shows the representative images of FGF7-stained (in red), collagen-I-stained (in green), and DAPI-stained (nuclear staining in blue) liver sections from healthy (Fig. 1C) and CCl_4 (Fig. 1D) mice. A strong increase in FGF7 expression can be seen in CCl_4-treated mice livers, which can be explained by the activation of HSCs during fibrogenesis as correlated with increased collagen-I expression. Furthermore, the expression of FGF7 (in red) colocalized with collagen-I matrix (in green), indicating the possible capture of HSCs-secreted FGF7 by the matrix (Fig. 1C-D). Furthermore, we investigated the expression of FGFR2b (in red), in combination with albumin (in green) as shown in Fig. 1E-F. We found that FGFR2b expression is increased in CCl_4-mice versus respective healthy controls as documented previously in early liver fibrosis [24,25]. Moreover, FGFR2b expression was mainly localized in damaged hepatocytes around the damaged areas (Fig. 1E-F).

Taken together, these results confirm the overexpression of FGF7 and FGFR2b during liver injury and that FGF7 and FGFR2b are expressed by HSCs and hepatocytes respectively.

3.2. Endogenous FGF7 treatment promotes hepatocyte proliferation

Several studies have proven that FGF7 promotes hepatic regeneration after partial hepatectomy [20] and hepatocyte survival during cholestatic liver injury [21]. In this study, we investigated if exogenous FGF7 treatment promotes hepatocyte proliferation following CCl_4-induced acute liver injury in mice. Liver injury was induced by 0.2 mL CCl_4/kg in C57BL/6 mice, followed by 2 days of treatment with 50 μg/kg FGF7 or vehicle twice daily (Fig. 2A). Liver sections from healthy, CCl_4, and CCl_4+ FGF7 mice were stained with Ki-67, a commonly used proliferation marker [27]. We found that the expression of Ki-67 was significantly upregulated ($p < 0.01$) in CCl_4 mice versus healthy controls indicating an initial response of repair after injury. FGF7-treated CCl_4 mice showed higher expression of Ki-67 versus vehicle-treated CCl_4 mice ($p < 0.05$) (Fig. 2B-C) indicating a pronounced proliferation effect upon exogenous FGF7 treatment. To confirm hepatocyte proliferation upon FGF7 treatment, we performed a fluorescent co-immunostaining with Ki-67 and albumin. Fig. 2D shows the co-localization of Ki-67 and albumin, indicating albumin-expressing hepatocytes proliferate upon FGF7 treatment.

To further validate hepatocyte proliferation upon FGF7 treatment, we performed in vitro studies and assessed cell viability using Alamar blue assays. Human hepatocytes (HepG2 cells) were treated with or without APAP for 24 h to mimic hepatocyte injury and were subsequently treated with 50 ng/mL FGF7 for 6 h (Fig. 2E). Results show increased cell viability indicative of increased cell proliferation following FGF7 treatment both in hepatocytes incubated with and without APAP (Fig. 2F).

Together these data suggest that treatment with FGF7 induces hepatocyte proliferation and/or improves cell viability in vitro and in vivo.

3.3. FGF7 improves hepatocyte survival by modulating various signalling pathways

Besides proliferation, increased cell viability via FGF7 can be caused by decreased cell apoptosis or improved cell survival by modulating signalling pathways and/or by increasing drug detoxification. To delineate the mechanisms involved, signalling pathway analysis using a mouse apoptosis signalling pathway phospho-antibody array was performed. We analysed 17 site-specific and phospho-specific antibodies (Supplementary Fig. S1A-B) i.e., AKT (P-Ser473), ATM (P-Ser1981), BAD (P-Ser112), Caspase-3 (P-Asp175), Caspase-7 (P-Asp198), CHK1 (P-Ser296), eIF-2a (P-Ser52), ERK1/2 (P-Thr202), HSP27 (P-Ser82), IKBa (P-Ser32), JNK (P-Thr183), NF-kB P65 (P-Ser536), p27 (P-Thr198), p38 (P-Thr180/Tyr182), P53 (P-Ser15), SMAD2 (P-Ser245) and TAK1 (P-Ser412) and quantified using AzureSpot Analysis Software. Many phospho-specific proteins showed differences as can be visualized in the heat map (Fig. 3A) and the nested plot and individual phospho-protein plots (Supplementary Fig. S1C-D), suggesting FGF7 controls multiple pathways in the liver. More prominently AKT, ERK, and P27 were significantly upregulated in FGF7-treated mice versus vehicle control (Fig. 3B). AKT and ERK pathways are known to regulate cell

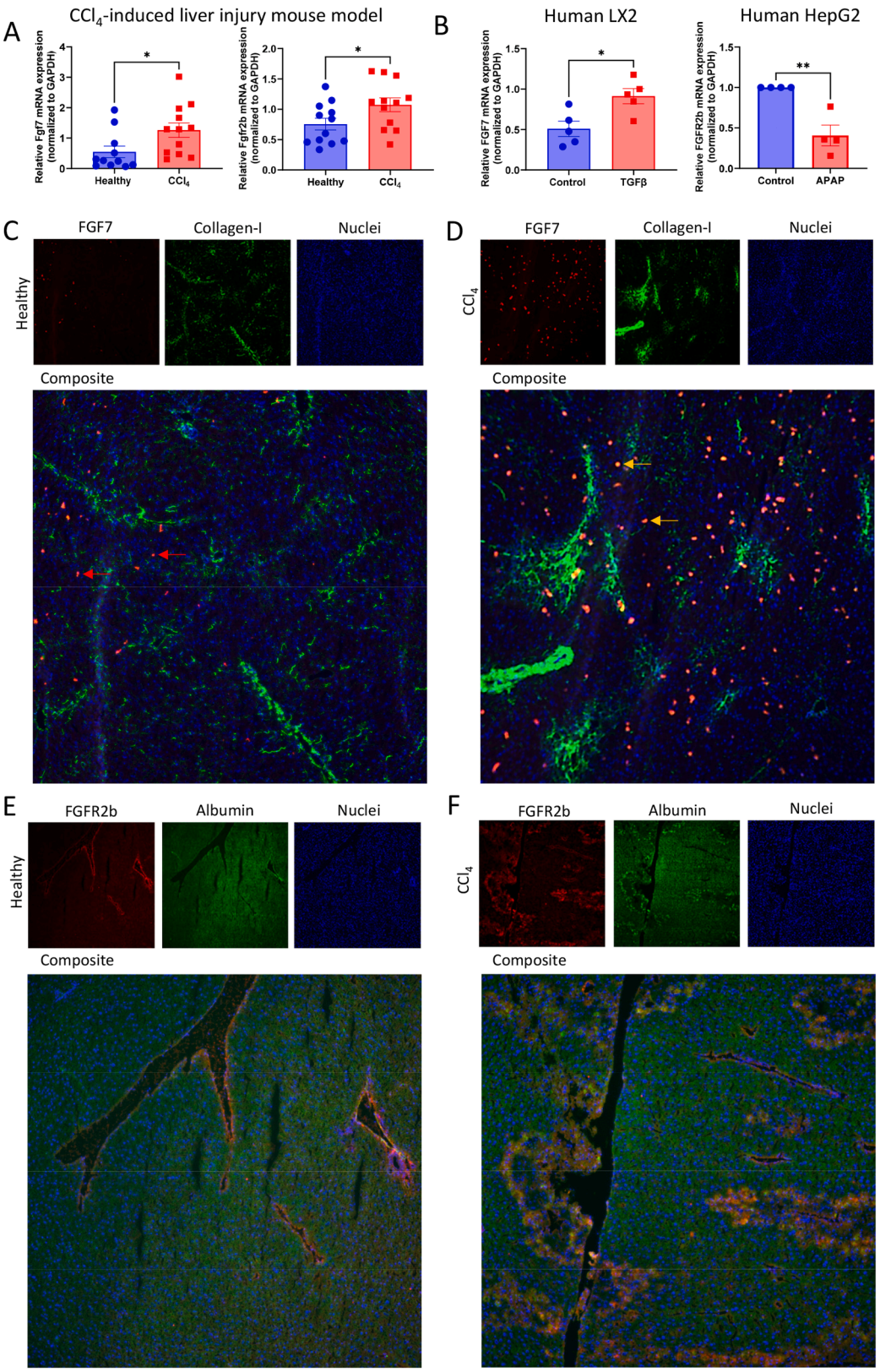

Fig. 1. The expression of FGF7 and FGFR2b in vivo and in vitro. (A) mRNA expression of Fgf7 and Fgfr2b in the healthy (n = 12) and acute CCl_4-induced liver injury mouse model (n = 12). (B) Relative mRNA expression of FGF7 (normalized with GAPDH) in control and TGF-β-activated hepatic stellate cells (n = 5). Relative mRNA expression FGFR2b (normalized with GAPDH) in control and APAP-treated hepatocytes (n = 5). (C and D) Representative (single-channel and composite) images of liver sections from healthy mice and mice with acute CCl_4-induced liver injury stained with FGF7 (red), Collagen-I (green), and DAPI (nuclear staining, blue). (E and F) Representative (single-channel and composite) images of liver sections from healthy mice and mice with acute CCl_4-induced liver injury stained with FGFR2 (red), Albumin (green), and DAPI (nuclear staining, blue). All results are presented as mean ± SEM; *p < 0.05, **p < 0.01; two-tailed t-test.

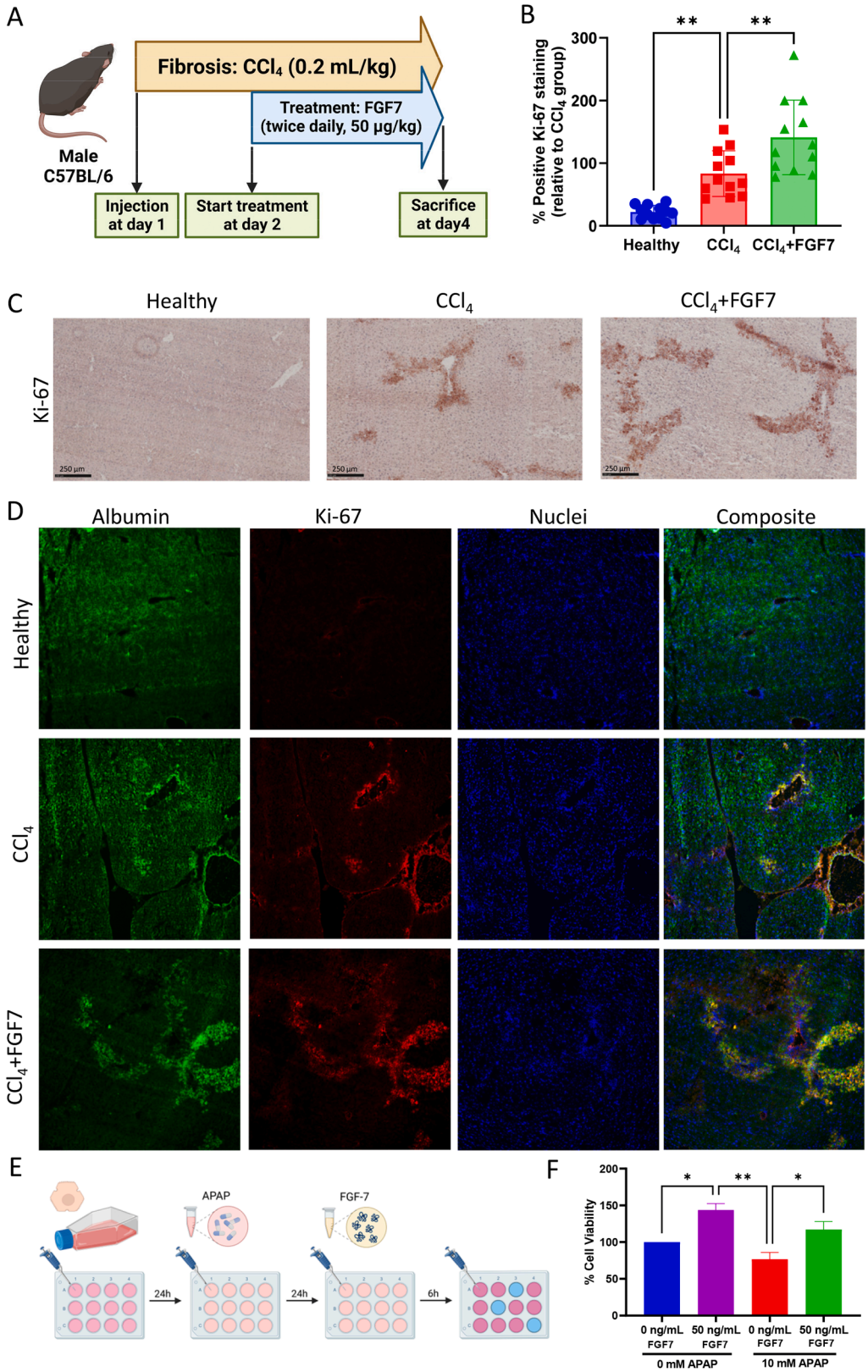

Fig. 2. The effect of FGF7 on hepatocyte proliferation in vivo and in vitro. (A) Schematic showing in vivo study design. (B) Quantitative analysis and (C) Representative images of liver section from healthy, CCl_4, and CCl_4 +FGF7 mice, n = 12 mice per group stained with Ki-67. (D) Representative images (single-channel and composite) of liver sections from healthy, CCl_4, and CCl_4 +FGF7 mice stained with Ki-67 (red), albumin (green), and DAPI (blue, nuclear staining). (E) Schematic showing in vitro viability study design performed in hepatocytes (HepG2). (F) Graph depicting % cell viability of HepG2 with and without APAP and FGF7 treatments from three independent experiments. All results are presented as mean ± SEM; *p < 0.05, **p < 0.01, and ***p < 0.001; One-way ANOVA with Bonferroni post-hoc test.

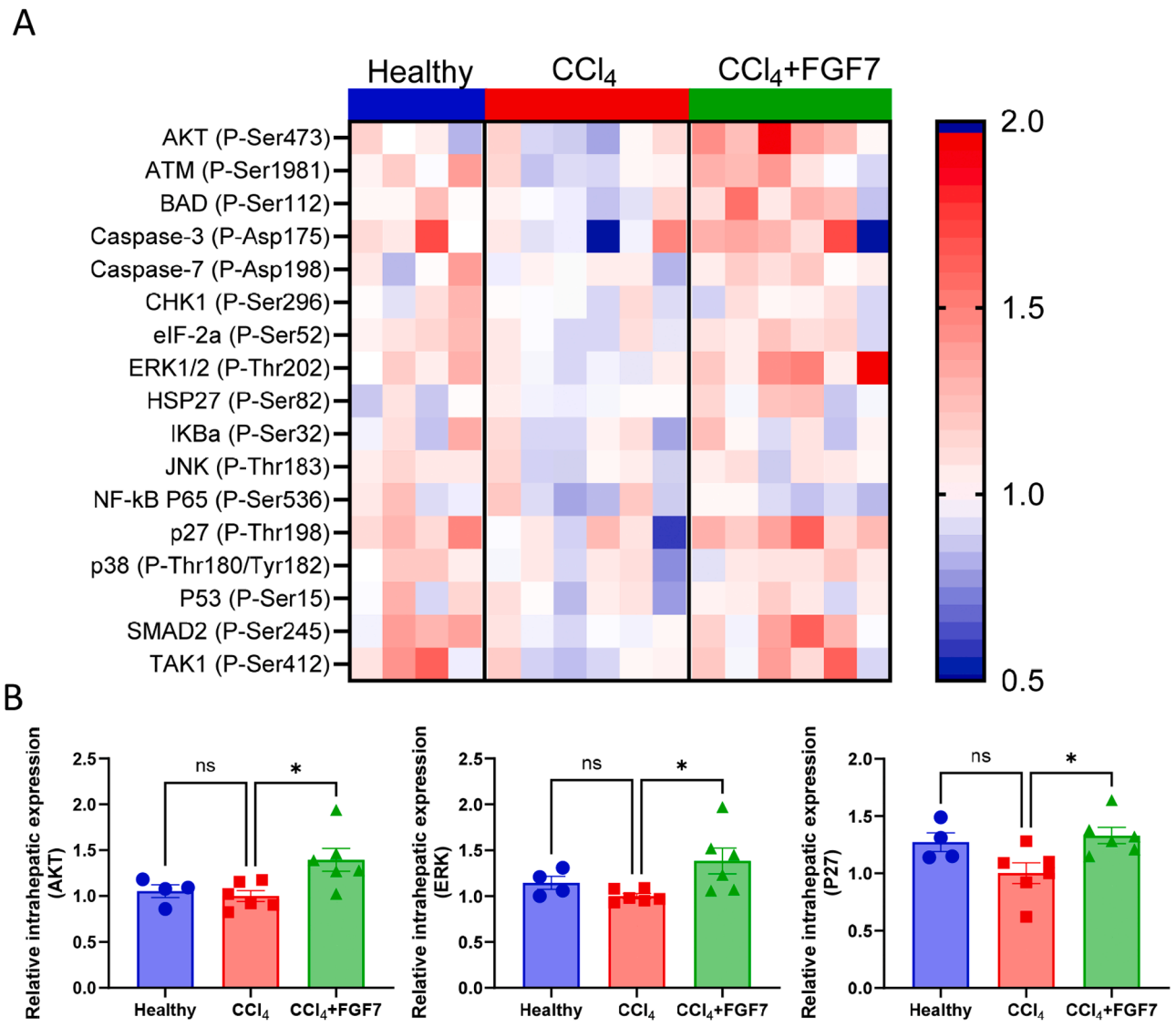

Fig. 3. The effect of FGF7 on hepatocyte survival is mediated via multiple signalling pathways in the liver. (A) Heatmap showing signalling pathway analysis results obtained from mouse apoptosis signalling pathway phospho-antibody array. Rows depict analysed phospho-proteins and columns depict mice groups (healthy, CCl_4, and CCl_4 +FGF7, n = 10–12); blue indicates lower expression and red indicates higher expression (normalized with reference positive control). (B) Relative intrahepatic expression of phosphoproteins (AKT, ERK, and P27, normalized with reference positive controls) in the liver tissues from healthy (n = 10), CCl_4 (n = 12), and CCl_4 +FGF7 (n = 12). Raw data and relative intrahepatic expression of other phosphoproteins (normalized with reference positive controls) are provided in Supplementary Fig. S1. All results are presented as mean ± SEM; *p < 0.05; One-way ANOVA with Bonferroni post-hoc test.

proliferation, and previous studies have shown that FGF-FGFR interaction activates multiple transduction pathways including ERK1/2, p38 and JNK kinase, and the PI3K-AKT pathway [18,28,29]. In this study, we observed that FGF7 activates AKT and ERK in accordance with previous studies [18,29]. Another protein that stood out in our analysis is p27 (Fig. 3B). P27 is expressed throughout the wild-type liver and is involved in maintaining hepatocyte quiescence [30]. Down-regulation of p27 indicates aberrant cell proliferation and increased p27 correlates with maintained hepatocyte quiescence and regulating uncontrolled proliferation causing carcinogenesis [30]. Notably, no significant differences were observed in the expression of phospho-specific proteins between healthy and vehicle control groups. This could be attributed to the fact that the changes in phosphorylated protein levels are generally short-lived. In this study, the CCl_4-administration was performed 72 h while FGF7 administration was performed less than 24 h before sacrificing.

Altogether, these results suggest the increased proliferation of hepatocytes via ERK and AKT pathways, while ensuring controlled hepatocyte proliferation without causing carcinogenesis via the p27 pathway.

We further analysed the expression of transcriptional regulators Albumin D-site-Binding protein (DBP), and thyrotrophic embryonic factor (TEF) that affect the expression of their target genes that encode for detoxifying cytochrome P450 enzymes [18]. Previous studies have shown that loss of *Dbp* and/or *Tef* in mice results in increased serum transaminase levels, impaired removal of pentobarbital, and enhanced toxicity of chemotherapeutics [18,31]. Moreover, it has been shown that FGF7 upregulates *Dbp* and *Tef* expression in wild-type mice and not in the *FgfR1/2*-albumin-specific knockout mice suggesting FGF7 via FGFR2b interaction controls drug detoxification in hepatocytes in the liver [18]. In this study, we show FGF7 upregulates *Dbp* and *Tef* gene expression (Fig. 4A) consistent with significant downregulation in plasma AST levels suggesting FGF7 promotes hepatic detoxification improving hepatocyte survival (Fig. 4B).

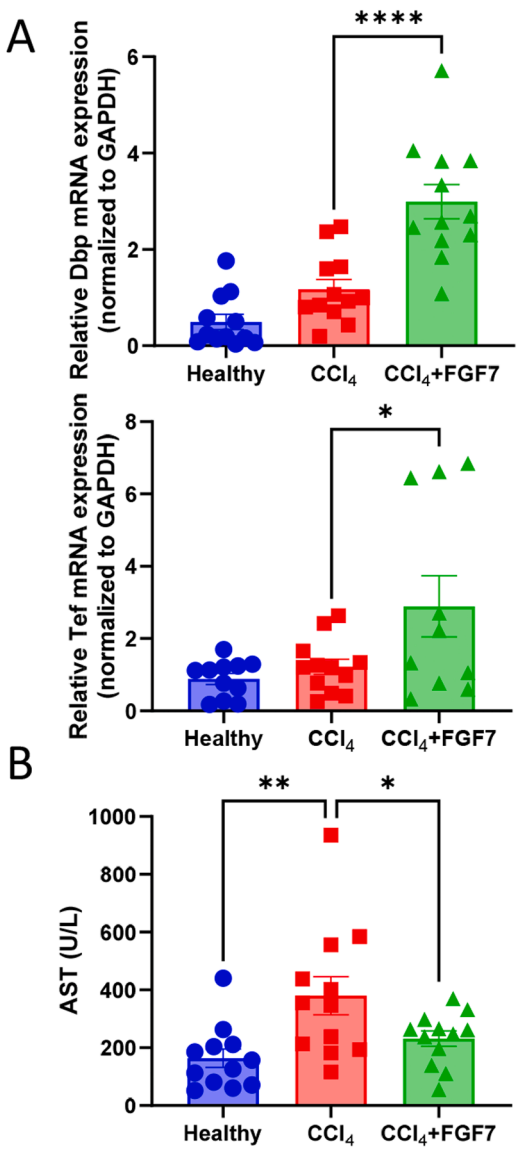

Fig. 4. The effect of FGF7 on hepatocyte drug detoxification. (A) Relative mRNA expression of *Dbp* and *Tef* (normalized to GAPDH) in the liver tissues from healthy, CCl_4, and CCl_4 +FGF7 mice, n = 10–12 mice per group. (B) Total AST levels in plasma from healthy, CCl_4, and CCl_4+FGF7 mice, n = 12 mice per group. All results are presented as mean ± SEM; *p < 0.05, **p < 0.01, and ****p < 0.0001; One-way ANOVA with Bonferroni post-hoc test.

3.4. FGF7 inhibits inflammation during acute liver injury via paracrine mechanisms

During liver injury, injured hepatocytes play a key role in inducing inflammation by secreting chemo-attractants, such as C-C motif chemokine ligand-2 (CCL-2), thereby inducing the recruitment of C-C motif chemokine receptor-2 (CCR2)-expressing monocytes [32]. Upon recruitment, these CCR-2 monocytes are activated into pro-inflammatory macrophages causing liver inflammation [33]. The surface markers expressed on these monocyte-derived macrophages (MoMFs) are different from the liver resident KCs. MoMFs are CD11b++ and F4/80+/-, while the KCs are F4/80++ and CD11b+/- [34]. Using flow cytometry, we identified and enumerated MoMFs and KCs in the liver tissues (Supplementary Fig. S2A-B). We observed a significant upregulation of the MoMFs in the vehicle-treated CCl_4 animals, which is significantly decreased upon FGF7 treatment (Fig. 5A-B). No significant differences in the number of KCs were observed in healthy, CCl_4, and CCl_4+FGF7 mice (Supplementary Fig. S2C).

We further analysed the total (F4/80-positive) macrophages and proinflammatory (iNOS-expressing) macrophages in the liver. A significant increase in F4/80 and iNOS expression was observed in the livers of CCl_4-mice compared with healthy controls, while a significant decrease in F4/80 and iNOS expression was evidenced in the FGF7-treated CCl_4-mice (Fig. 5C-D).

To confirm if the effects observed on liver inflammation in vivo are due to the paracrine effects of FGF7-treated hepatocytes, we analysed the mRNA expression of chemoattractant CCL2 and pro-inflammatory CXCL8 (interleukin-8, IL-8) in hepatocytes incubated with 10 mM APAP. Corroborated with previous studies [35], hepatocytes incubated with APAP showed higher expression of CCL2 and CXCL8 (Fig. 5E). FGF7 treatment post-APAP-induced hepatocyte injury led to a significant decrease in CCL2 and CXCL8 expression (Fig. 5E) suggesting a paracrine effect of FGF7-treated hepatocytes on liver inflammation.

3.5. FGF7 inhibits fibrogenesis during acute liver injury via paracrine mechanisms

Following liver injury, damaged hepatocytes and inflammatory macrophages secrete profibrotic (paracrine) factors e.g., PDGFβ and TGFβ that lead to the proliferation and activation of HSCs respectively. HSCs upon activation secrete large amounts of ECM mainly collagen-I. We hypothesized that injured hepatocytes activate HSCs while FGF7 treatment will inhibit (TGFβ-induced) HSCs activation via paracrine mechanisms.

Indeed, we observed increased collagen-I (a major ECM protein secreted by HSCs) and alpha-smooth muscle actin (α-SMA, HSCs activation marker) expression in the livers of CCl_4-mice (Fig. 6A-B), and FGF7 treatment inhibited the expression of collagen-I and α-SMA (Fig. 6A-B) indicating paracrine effects of FGF7. This inhibition could be a consequence of inhibition in macrophage infiltration and activation as observed previously (Fig. 5) and improved hepatocyte viability/survival resulting in reduced secretion of profibrogenic factors attenuating HSCs proliferation and activation.

To evaluate if these HSCs-inhibitory effects are mediated partially via FGF7-treated hepatocytes, we performed conditioned medium studies. We induced hepatocyte injury by APAP and treated APAP-hepatocytes with FGF7 (Supplementary Fig. S3). We collected the conditioned medium from the hepatocytes (APAP-hepatocytes ± FGF7) and incubated LX-2 cells (human HSCs) with a 2:1 (conditioned: fresh medium) and investigated the collagen-I gene expression. We found that LX-2 cells treated with conditioned medium from APAP+FGF7-treated hepatocytes showed a significant reduction in collagen-I expression, compared to LX-2 cells treated with medium from APAP-treated hepatocytes that did not receive FGF7 treatment (Fig. 6C). No differences in TGFβ gene expression were observed in hepatocytes suggesting that these effects are mediated via other paracrine factors secreted by hepatocytes (hepatokines).

3.6. FGF7 treatment shows no severe adverse effects

To determine possible side-effects of FGF7, we analysed the body weight and organ-to-body weight of five vital organs: liver, lungs, kidneys, spleen, and heart (Supplementary Fig. S4). No significant differences in body weight were found between healthy, CCl_4-mice, and CCl_4 +FGF7-treated mice. FGF7 treatment showed improved body weight change compared to CCl_4-mice (non-significant) (Supplementary Fig. S4). During liver injury, the liver-to-body weight was increased significantly, and FGF7 treatment did not show any effects on liver weight. Lastly, no significant changes have been found in any other organ, except the spleen which might be due to an increase in the number of splenocytes as shown previously [36].

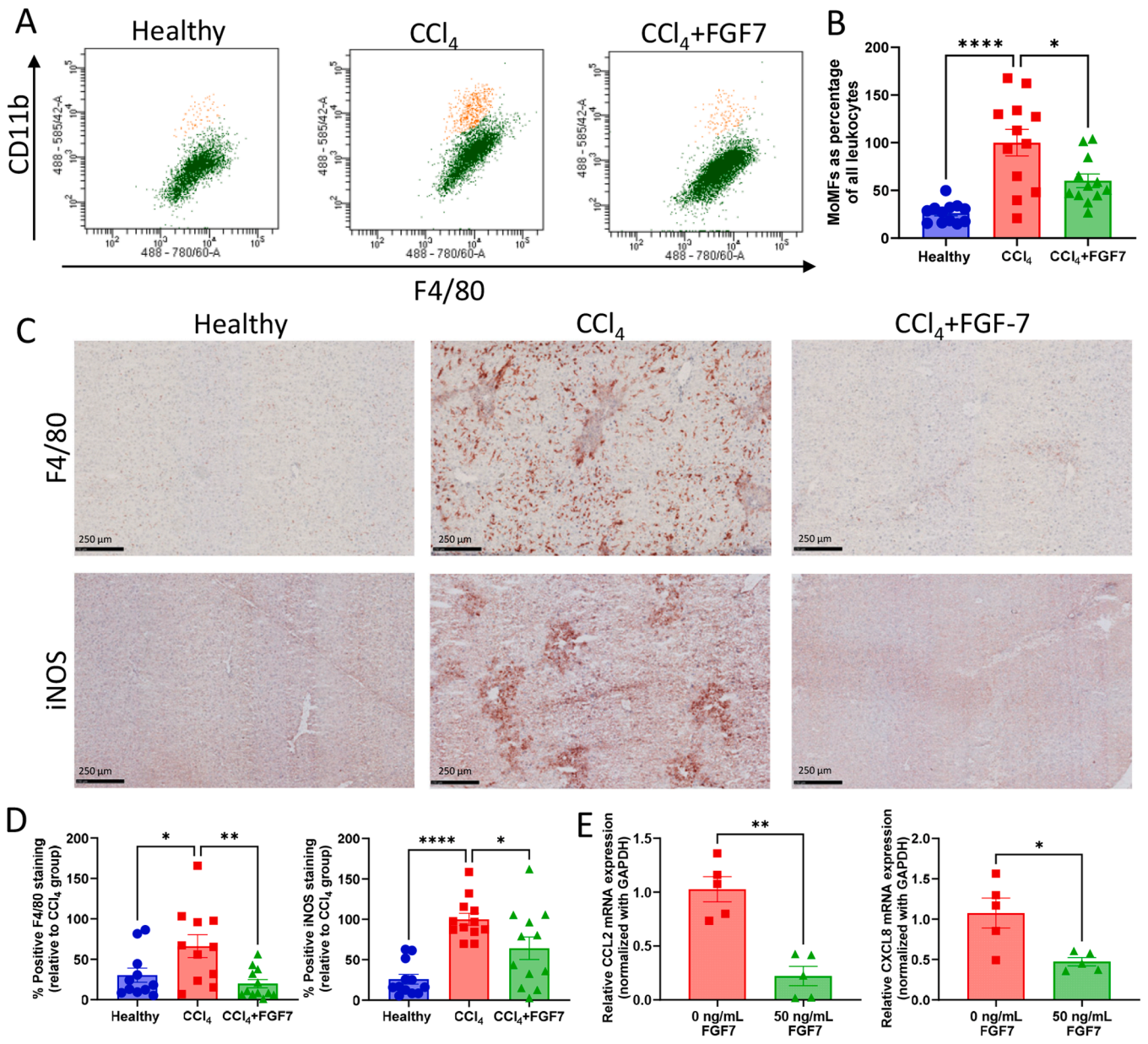

Fig. 5. Paracrine effects of FGF7 on macrophage recruitment and inflammation. (A) Representative flow plots showing CD11b-expressing CD45+ leukocytes on the y-axis and F4/80-expressing CD45+ leukocytes on the x-axis. Monocyte-derived macrophages (MoMFs) were identified as CD11b++ and F4/80+/-, and KCs were identified as CD11b+/- and F4/80++ (refer to Fig. S2 for the workflow and gating strategy). (B) Quantitative analysis of MoMFs (indicated with orange colour) as a percentage of all leukocytes (CD45+). (C) Representative images and (D) quantitative analysis of F4/80 and iNOS antibody-stained liver sections from healthy, CCl_4, and CCl_4+FGF7 mice, n = 12 mice per group. (E) CCL2 and CXCL8 gene expression (normalized with GAPDH) in HepG2 cells treated with 10 mM APAP ± 50 ng/mL FGF7 (5 independent experiments). All results are presented as mean ± SEM; *$p < 0.05$, **$p < 0.01$, and ****$p < 0.0001$; One-way ANOVA with Bonferroni post-hoc test (B and D), two-tailed t-test (E).

4. Discussion

In this study, we investigated the therapeutic potential of FGF7 in promoting hepatocyte survival and proliferation, thereby ameliorating inflammation and fibrosis via paracrine mechanisms during acute liver injury. We first examined the expression of *Fgf7* and *FgfR2b* during acute liver injury in mice and found the expression of *Fgf7* as well as *FgfR2b* to be upregulated in liver disease. Steiling et al. reported that primary murine and human HSCs produce FGF7 [24]. On the other hand, Takase et al. showed that Thy-1-expressing cells also produce FGF7 [21]. These Thy-1-expressing cells are portal fibroblasts, that infiltrate the liver during acute liver injury and contribute to liver fibrogenesis [37]. In accordance with the previous studies [21,24,37], we observed that co-staining of FGF7 and collagen-I revealed that FGF7 is expressed by HSCs (and portal fibroblasts). We further show that FGFR2b is expressed by hepatocytes in vivo during acute liver as shown previously [24]. Additionally, we assessed the expression of FGF7 in LX-2 (human HSCs) and FGFR2b in HepG2 (human hepatocytes). In LX-2, we found a similar upregulation of FGF7 after TGF-β activation, supporting the hypothesis that these cells express FGF7 upon activation during liver injury [38]. Interestingly, FGFR2b expression was decreased in HepG2 upon APAP-induced damage. This decrease could be explained by decreased cell viability and increased apoptosis, resulting in a reduced cell number and reduced FGFR2b expression.

Next, we investigated the therapeutic potential of FGF7 in an acute CCl_4-induced liver injury mouse model. We first investigated the effect

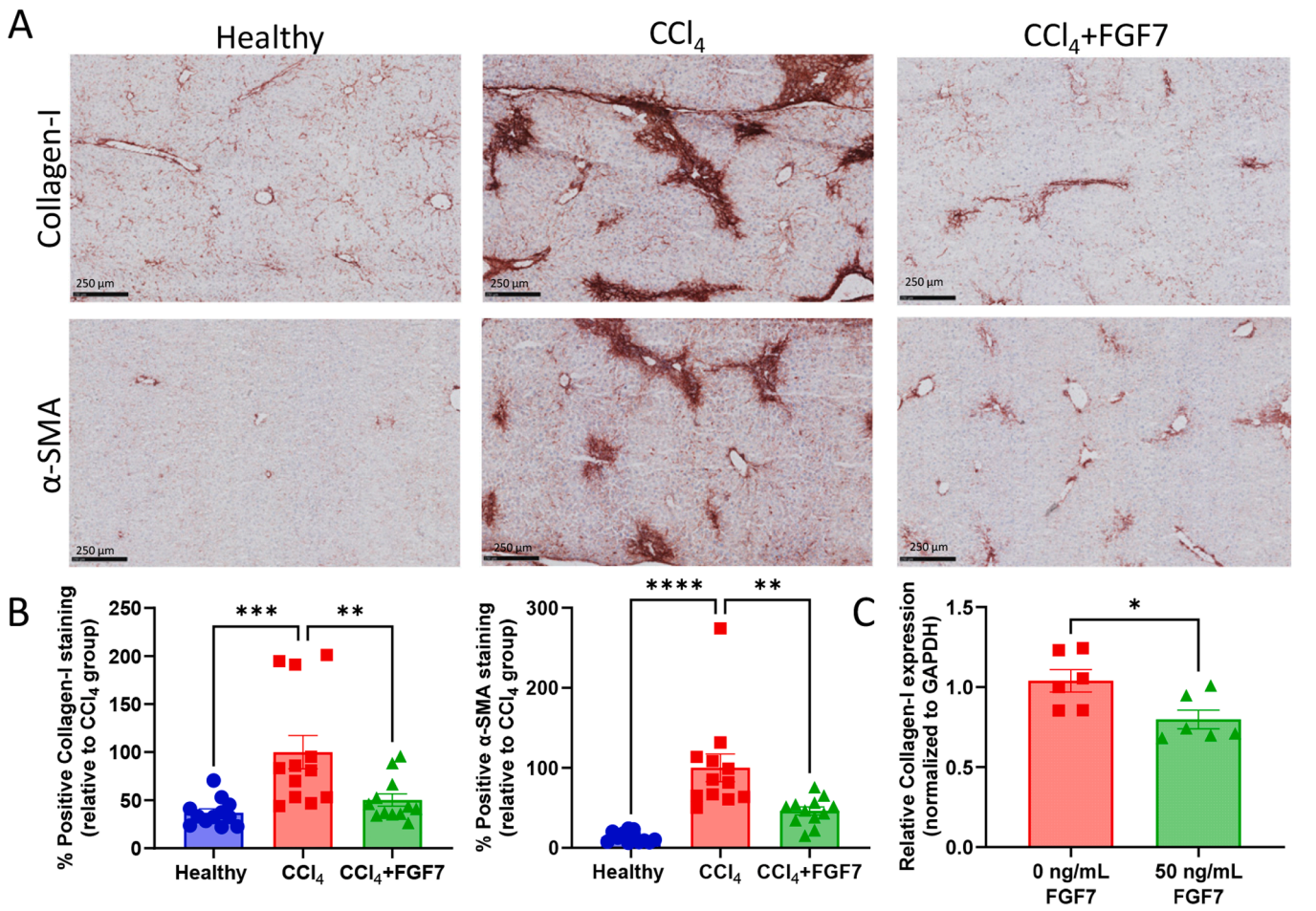

Fig. 6. Paracrine effects of FGF7 on HSCs activation, and fibrogenesis. (A) Representative images and (B) quantitative analysis of collagen-I- and α-SMA-stained liver sections from healthy, CCl_4, and CCl_4 +FGF7 mice (n = 12 mice per group). (C) Relative collagen-I gene expression (normalized to GAPDH) of LX-2 cells treated with conditioned medium obtained from HepG2 treated with 10 mM APAP ± 50 ng/mL FGF7. All results are presented as mean ± SEM; *p < 0.05, **p < 0.01, ***p < 0.001, and ****p < 0.0001; One-way ANOVA with Bonferroni post-hoc test (B), two-tailed t-test (C).

of FGF7 treatment on hepatocyte proliferation as shown in a mouse model of partial hepatectomy [20]. We analysed the Ki-67 (a proliferation marker) expression in healthy, vehicle-treated, and FGF7-treated CCl_4-mice livers. Takase et al. showed that Fgf7 knock-out animals showed decreased Ki67 expression, thereby implicating that Fgf7 is involved in proliferation as visualized by Ki-67 staining [21]. This is in line with our data showing an increasing Ki-67 expression in FGF7-treated CCl_4-mice. The co-immunofluorescent staining shows the localization of Ki-67 with albumin indicating proliferation of hepatocytes. This proliferation was further confirmed in vitro using an Alamar blue assay where we observed that FGF7 treatment improved HepG2 cell viability with and without APAP treatment suggesting that FGF7 induces hepatocyte proliferation. We further delineated the mechanisms involved in FGF7-induced effects on hepatocytes, we analysed a panel of 17 phosphoproteins involved in cell apoptosis/proliferation. We observed several pathways are regulated by FGF7, however, more prominently, a significant upregulation of extracellular signal-regulated kinase (ERK) and protein kinase B (AKT) phosphoproteins were observed suggesting increased activation of ERK and AKT signalling pathways resulting in improved cell proliferation. This upregulation has been reported and the precursory cascade has also been elucidated. The binding of FGF7 to FGFR2b leads to the activation of a signalling cascade starting with FGFR substrate 2α (FRS2α) and growth factor receptor-bound-2 (GBR2) that activates AKT pathway via phosphatidylinositol 3-kinase (Pi3K) [17,29] and ERK pathway via reticular activating system (RAS) [39,40].

Furthermore, it has been shown that FGFR2 deletion leads to reduced expression of P27, which was correlated with increased apoptosis [41,42]. This suggests a protective effect of FGFR2 on hepatocytes via P27, which we also observed in this study. On the other hand, P27 is a key inhibitor of the cell cycle and proliferation, thereby sustaining a quiescent state [30]. P27 upregulation could indicate improved hepatocyte survival and maintained hepatocyte quiescence regulating uncontrolled proliferation and carcinogenesis. As reported previously FGF7 also increases the expression of transcription factors *Dbp* and *Tef* [18] that regulate the expression of hepatic detoxifying enzymes and metabolic activity [43,44], we also analysed the expression of *Dbp* and *Tef* in vivo in acute injury mouse livers. We found increased expression of these transcription factors upon FGF7 treatment and reduced AST levels suggesting that FGF7 promotes hepatic detoxification further improving hepatocyte survival.

We next examined the paracrine effects of (FGF7-treated) hepatocytes on inflammation and fibrosis. Damaged hepatocytes release paracrine factors (hepatokines) e.g., chemoattractants such as CCL2 and CXCL8/IL-8 to induce recruitment of CCR2 expressing circulating monocytes and neutrophils respectively [32]. Upon recruitment, these monocytes differentiate into macrophages (MoMFs) and contribute to liver inflammation together with other immune cells including neutrophils [33]. We hypothesized that FGF7-induced hepatocyte survival and proliferation would decrease the expression of these inflammatory hepatokines attenuating infiltration of immune cells and inflammation. To examine this hypothesis, using flow cytometry analysis, we first

analysed the infiltrated monocyte (CD11b++ F4/80+/-) population populations [34,45], and found a significant upregulation of MoMFs in the vehicle-treated animals, which was significantly decreased upon FGF7 treatment indicating that improved hepatocyte survival leads to decreased infiltration of MoMFs. No significant effect of FGF7 treatment was observed on the resident macrophages (KCs). These results were further confirmed by immunostainings using F4/80 (pan-macrophage marker) and iNOS (pro-inflammatory macrophage marker) which was inhibited by FGF7 treatment. To further analyse if this effect is indeed mediated by reduced hepatocyte-chemokine (hepatokine) levels, we analysed the mRNA expression of major chemokines secreted by hepatocytes i.e., CCL2 and CXCL8 in APAP-injured HepG2 cells with and without FGF7 treatment in vitro. The expression of CCL2 and CXCL8 was significantly decreased upon FGF7 treatment, emphasizing the role of hepatocyte survival in ameliorating immune cell infiltration and liver inflammation.

Hepatocyte injury induces fibrosis via necrosis products [46] and indirectly via activation of inflammatory cells, which subsequently activate HSCs [47]. It has been investigated that hepatocyte survival can reduce portal hypertension and ameliorate fibrosis [48]. Here, we investigated if FGF7-induced cell survival leads to decreased fibrosis via paracrine mechanisms. In vivo in the CCl_4-induced acute liver injury model, we observed a significant decrease in collagen-I and α-SMA expression indicating reduced fibrosis. To further investigate the paracrine effect of hepatocyte survival on HSCs, we performed conditioned medium studies where LX-2 cells were incubated with conditioned medium from APAP-injured HepG2 with and without FGF7 treatment. Conditioned medium from APAP-HepG2 cells treated with FGF7 showed a significant reduction in collagen-I expression suggesting paracrine effects of hepatocytes on HSCs [49]. This could be attributed to the reduced secretion of pro-fibrotic hepatokines by hepatocytes [50] upon FGF7 treatment.

One of the limitations of our study is the use of acute livery injury mouse model (due to ethical reasons) that does not correspond to the clinical situation. Patients normally present to the clinic when liver damage progresses to chronic-to-advanced liver disease. More studies are hence warranted in different (etiological) liver disease models to examine the therapeutic potential of FGF7-therapy.

In conclusion, in this study, we have successfully analysed the therapeutic potential of FGF7 treatment in acute liver injury. FGF7-induced hepatocyte survival and proliferation mediated via multiple signalling pathways ameliorated liver inflammation and fibrosis via paracrine mechanisms. This study warrants the exploration of FGF7, FGF7 derivatives, nano-engineered FGF7, or FGFR2b agonists for further development and for future clinical applications driving hepatocyte and liver regeneration.

CRediT authorship contribution statement

Eline Geervliet: Methodology, Investigation, Validation, Visualization, Data curation, Writing – original draft. **Leon WMM Terstappen:** Resources, Data curation, Supervision, Writing – review & editing. **Ruchi Bansal:** Conceptualization, Methodology, Formal analysis, Resources, Data curation, Writing – review & editing, Visualization, Supervision, Project administration, Funding acquisition.

Declaration of Competing Interest

The authors declare that they have no known competing financial interests or personal relationships that could have appeared to influence the work reported in this paper.

Acknowledgements

The authors acknowledge the support of Franck Assayag in animal studies. We acknowledge the financial support of the EASL in the form of Juan Rodés Ph.D. Student Fellowship (awarded to EG), and the financial support provided by the University of Twente, The Netherlands. We also acknowledge the TLR-MCBP team for active scientific discussions during the study.

Appendix A. Supporting information

Supplementary data associated with this article can be found in the online version at doi:10.1016/j.biopha.2023.115612.

References

[1] T. Luedde, N. Kaplowitz, R.F. Schwabe, Cell death and cell death responses in liver disease: mechanisms and clinical relevance, Gastroenterology 147 (4) (2014) 765–783.e4.
[2] C. Trautwein, A. Koch, Mechanisms of acute liver failure, Liver Immunol.: Princ. Pract. (2013) 373–388.
[3] J.S. Roh, D.H. Sohn, Damage-associated molecular patterns in inflammatory diseases, Immune Netw. 18 (4) (2018), e27.
[4] S.Y. Neshat, et al., Liver disease: induction, progression, immunological mechanisms, and therapeutic interventions, Int. J. Mol. Sci. 22 (13) (2021).
[5] F. Tacke, C. Trautwein, Mechanisms of liver fibrosis resolution, J. Hepatol. 63 (4) (2015) 1038–1039.
[6] P. Ramachandran, J.P. Iredale, J.A. Fallowfield, Resolution of liver fibrosis: basic mechanisms and clinical relevance, Semin. Liver Dis. 35 (2) (2015) 119–131.
[7] R. Bansal, K. Poelstra, Hepatic stellate cell targeting using peptide-modified biologicals, Methods Mol. Biol. 2669 (2023) 269–284.
[8] E. Geervliet, et al., Matrix metalloproteinase-1 decorated polymersomes, a surface-active extracellular matrix therapeutic, potentiates collagen degradation and attenuates early liver fibrosis, J. Control Release 332 (2021) 594–607.
[9] R. Bansal, B. Nagorniewicz, J. Prakash, Clinical advancements in the targeted therapies against liver fibrosis, Mediat. Inflamm. 2016 (2016), 7629724.
[10] P. Burra, et al., Limitations of current liver donor allocation systems and the impact of newer indications for liver transplantation, J. Hepatol. 75 (2021) S178–S190.
[11] J.F. Trotter, Sirolimus in liver transplantation, Transplant. Proc. 35 (3, Supplement) (2003) S193–S200.
[12] M.R. Dewhurst, et al., Loss of hepatocyte cell division leads to liver inflammation and fibrosis, PLoS Genet. 16 (11) (2020), e1009084.
[13] H. Malhi, M.E. Guicciardi, G.J. Gores, Hepatocyte death: a clear and present danger, Physiol. Rev. 90 (3) (2010) 1165–1194.
[14] L.A. Lee, Advances in hepatocyte transplantation: a myth becomes reality, J. Clin. Invest. 108 (3) (2001) 367–369.
[15] X. Lin, et al., miR-155 accelerates proliferation of mouse hepatocytes during liver regeneration by directly targeting SOCS1, Am. J. Physiol. Gastrointest. Liver Physiol. 315 (4) (2018) G443–G453.
[16] S. Padrissa-Altés, et al., Control of hepatocyte proliferation and survival by Fgf receptors is essential for liver regeneration in mice, Gut 64 (9) (2015) 1444–1453.
[17] T. Seitz, C. Hellerbrand, Role of fibroblast growth factor signalling in hepatic fibrosis, Liver Int. 41 (6) (2021) 1201–1215.
[18] F. Bohm, et al., FGF receptors 1 and 2 control chemically induced injury and compound detoxification in regenerating livers of mice, Gastroenterology 139 (4) (2010) 1385–1396.
[19] D.W. Kurniawan, et al., Fibroblast growth factor 2 conjugated superparamagnetic iron oxide nanoparticles (FGF2-SPIONs) ameliorate hepatic stellate cells activation in vitro and acute liver injury in vivo, J. Control Release 328 (2020) 640–652.
[20] S.M. Tsai, W.P. Wang, Expression and function of fibroblast growth factor (FGF) 7 during liver regeneration, Cell Physiol. Biochem. 27 (6) (2011) 641–652.
[21] H.M. Takase, et al., FGF7 is a functional niche signal required for stimulation of adult liver progenitor cells that support liver regeneration, Genes Dev. 27 (2) (2013) 169–181.
[22] Z. Sun, et al., Fibroblast growth factor 7 inhibits cholesterol 7alpha-hydroxylase gene expression in hepatocytes, Biochem. Biophys. Res. Commun. 423 (4) (2012) 775–780.
[23] T. Amann, et al., Reduced expression of fibroblast growth factor receptor 2IIIb in hepatocellular carcinoma induces a more aggressive growth, Am. J. Pathol. 176 (3) (2010) 1433–1442.
[24] H. Steiling, et al., Activated hepatic stellate cells express keratinocyte growth factor in chronic liver disease, Am. J. Pathol. 165 (4) (2004) 1233–1241.
[25] J.M. Otte, et al., Differential regulated expression of keratinocyte growth factor and its receptor in experimental and human liver fibrosis, Regul. Pept. 144 (1–3) (2007) 82–90.
[26] T. Amann, et al., Reduced expression of fibroblast growth factor receptor 2IIIb in hepatocellular carcinoma induces a more aggressive growth, Am. J. Pathol. 176 (3) (2010) 1433–1442.
[27] K.D. Kaita, N. Pettigrew, G.Y. Minuk, Hepatic regeneration in humans with various liver disease as assessed by Ki-67 staining of formalin-fixed paraffin-embedded liver tissue, Liver 17 (1) (1997) 13–16.
[28] L. Dailey, et al., Mechanisms underlying differential responses to FGF signaling, Cytokine Growth Factor Rev. 16 (2) (2005) 233–247.
[29] S. Utley, et al., Fibroblast growth factor signaling regulates the expansion of A6-expressing hepatocytes in association with AKT-dependent β-catenin activation, J. Hepatol. 60 (5) (2014) 1002–1009.

[30] Y.H. Kwon, et al., P21 functions to maintain quiescence of p27-deficient hepatocytes, J. Biol. Chem. 277 (44) (2002) 41417–41422.
[31] F. Gachon, et al., The circadian PAR-domain basic leucine zipper transcription factors DBP, TEF, and HLF modulate basal and inducible xenobiotic detoxification, Cell Metab. 4 (1) (2006) 25–36.
[32] Z. Zhou, M.J. Xu, B. Gao, Hepatocytes: a key cell type for innate immunity, Cell Mol. Immunol. 13 (3) (2016) 301–315.
[33] S. She, et al., Functional roles of chemokine receptor CCR2 and its ligands in liver disease, Front. Immunol. 13 (2022), 812431.
[34] J.C. Mossanen, et al., Chemokine (C-C motif) receptor 2-positive monocytes aggravate the early phase of acetaminophen-induced acute liver injury, Hepatology 64 (5) (2016) 1667–1682.
[35] Y. Saiman, S.L. Friedman, The role of chemokines in acute liver injury, Front. Physiol. 3 (2012) 213.
[36] K. Yakimchuk, et al., Keratinocyte growth factor (KGF) delays the onset of collagen-induced arthritis, Autoimmunity 45 (7) (2012) 510–515.
[37] L.W. Katsumata, A. Miyajima, T. Itoh, Portal fibroblasts marked by the surface antigen Thy1 contribute to fibrosis in mouse models of cholestatic liver injury, Hepatol. Commun. 1 (3) (2017) 198–214.
[38] C. Wang, et al., Disruption of FGF signaling ameliorates inflammatory response in hepatic stellate cells, Front. Cell Dev. Biol. 8 (2020) 601.
[39] Y.M. Jeon, et al., Fibroblast growth factor-7 facilitates osteogenic differentiation of embryonic stem cells through the activation of ERK/Runx2 signaling, Mol. Cell Biochem. 382 (1–2) (2013) 37–45.
[40] J. Klufa, et al., Hair eruption initiates and commensal skin microbiota aggravate adverse events of anti-EGFR therapy, Sci. Transl. Med. 11 (522) (2019), eaax2693.
[41] C.M. Garcia, et al., Signaling through FGF receptor-2 is required for lens cell survival and for withdrawal from the cell cycle during lens fiber cell differentiation, Dev. Dyn. 233 (2) (2005) 516–527.
[42] H. Zhao, et al., Fibroblast growth factor receptor signaling is essential for lens fiber cell differentiation, Dev. Biol. 318 (2) (2008) 276–288.
[43] N. Allaman-Pillet, et al., Circadian regulation of islet genes involved in insulin production and secretion, Mol. Cell Endocrinol. 226 (1–2) (2004) 59–66.
[44] M. Stratmann, et al., Flexible phase adjustment of circadian albumin D site-binding protein (DBP) gene expression by CRYPTOCHROME1, Genes Dev. 24 (12) (2010) 1317–1328.
[45] T. Puengel, et al., Differential impact of the dual CCR2/CCR5 inhibitor cenicriviroc on migration of monocyte and lymphocyte subsets in acute liver injury, PLoS One 12 (9) (2017), e0184694.
[46] A. Caligiuri, et al., Cellular and molecular mechanisms underlying liver fibrosis regression, Cells 10 (10) (2021).
[47] E. Seki, R.F. Schwabe, Hepatic inflammation and fibrosis: functional links and key pathways, Hepatology 61 (3) (2015) 1066–1079.
[48] J. Gracia-Sancho, et al., Emricasan ameliorates portal hypertension and liver fibrosis in cirrhotic rats through a hepatocyte-mediated paracrine mechanism, Hepatol. Commun. 3 (7) (2019) 987–1000.
[49] A. Zisser, D.H. Ipsen, P. Tveden-Nyborg, Hepatic stellate cell activation and inactivation in NASH-fibrosis—roles as putative treatment targets? Biomedicines 9 (4) (2021) 365.
[50] A. Loft, et al., Liver-fibrosis-activated transcriptional networks govern hepatocyte reprogramming and intra-hepatic communication, Cell Metab. 33 (8) (2021) 1685–1700, e9.